AD-A126 482 TENSILE PROPERTY EVALUATION OF POLYCRYSTALLINE ALUMINA FILAMENTS AND THEIR COMPOSITES(U) ARMY MATERIALS AND MECHANICS RESEARCH CENTER WATERTOWN MA J NUNES DEC 82 1/1

UNCLASSIFIED AMMRC-TR-82-61 F/G 11/4 NL

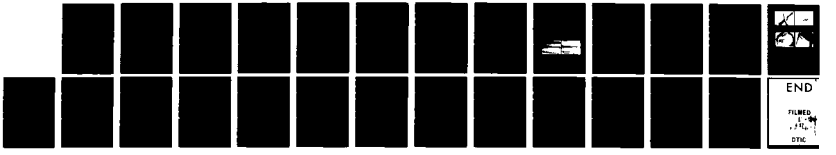

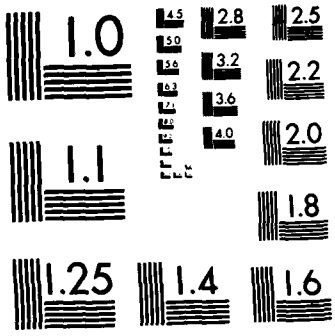

MICROCOPY RESOLUTION TEST CHART
NATIONAL BUREAU OF STANDARDS-1963-A

AMMRC TR 82-61

(12

AD

AD A126482

TENSILE PROPERTY EVALUATION OF POLYCRYSTALLINE ALUMINA FILAMENTS AND THEIR COMPOSITES

JOHN NUNES
METALS RESEARCH DIVISION

December 1982

ARMY MATERIALS AND MECHANICS RESEARCH CENTER
Watertown, Massachusetts 02172

The findings in this report are not to be construed as an official Department of the Army position, unless so designated by other authorized documents.

Mention of any trade names or manufacturers in this report shall not be construed as advertising nor as an official endorsement or approval of such products or companies by the United States Government.

UNCLASSIFIED

SECURITY CLASSIFICATION OF THIS PAGE (When Data Entered)

REPORT DOCUMENTATION PAGE		READ INSTRUCTIONS BEFORE COMPLETING FORM
1. REPORT NUMBER AMMRC TR 82-61	2. GOVT ACCESSION NO. A126482	3. RECIPIENT'S CATALOG NUMBER
4. TITLE (and Subtitle) TENSILE PROPERTY EVALUATION OF POLYCRYSTALLINE ALUMINA FILAMENTS AND THEIR COMPOSITES		5. TYPE OF REPORT & PERIOD COVERED Final Report 6. PERFORMING ORG. REPORT NUMBER
7. AUTHOR(s) John Nunes		8. CONTRACT OR GRANT NUMBER(s)
9. PERFORMING ORGANIZATION NAME AND ADDRESS Army Materials and Mechanics Research Center Watertown, Massachusetts 02172 DRXMR-MM		10. PROGRAM ELEMENT, PROJECT, TASK AREA & WORK UNIT NUMBERS D/A Project: IL162105AH84 AMCMS Code: 612105.11.H84
11. CONTROLLING OFFICE NAME AND ADDRESS U. S. Army Materiel Development and Readiness Command, Alexandria, Virginia 22333		12. REPORT DATE December 1982 13. NUMBER OF PAGES 21
14. MONITORING AGENCY NAME & ADDRESS(if different from Controlling Office)		15. SECURITY CLASS. (of this report) Unclassified 15a. DECLASSIFICATION/DOWNGRADING SCHEDULE

16. DISTRIBUTION STATEMENT (of this Report)

Approved for public release; distribution unlimited.

17. DISTRIBUTION STATEMENT (of the abstract entered in Block 20, if different from Report)

18. SUPPLEMENTARY NOTES

19. KEY WORDS (Continue on reverse side if necessary and identify by block number)

Composite materials	Aluminum oxides	Statistical analysis
Metal matrix composites	Polycrystalline	Aluminum
Fiber reinforced composites	Tensile properties	Ceramic fibers

20. ABSTRACT (Continue on reverse side if necessary and identify by block number)

(SEE REVERSE SIDE)

DD FORM 1 JAN 73 1473 EDITION OF 1 NOV 65 IS OBSOLETE

UNCLASSIFIED

SECURITY CLASSIFICATION OF THIS PAGE (When Data Entered)

Block No. 20

ABSTRACT

The tensile properties of polycrystalline alumina filaments (DuPont Fiber FP) were experimentally measured and statistically evaluated for several different gage lengths (0.5, 1, 2, 3, 5, and 10 inches).

Using a two-parameter Weibull distribution function to describe the in situ filament failure stresses, a statistical failure mode analysis for composites gave excellent agreement between theoretical predictions and published tensile strength data on cast Fiber FP/aluminum and Fiber FP/magnesium.

CONTENTS

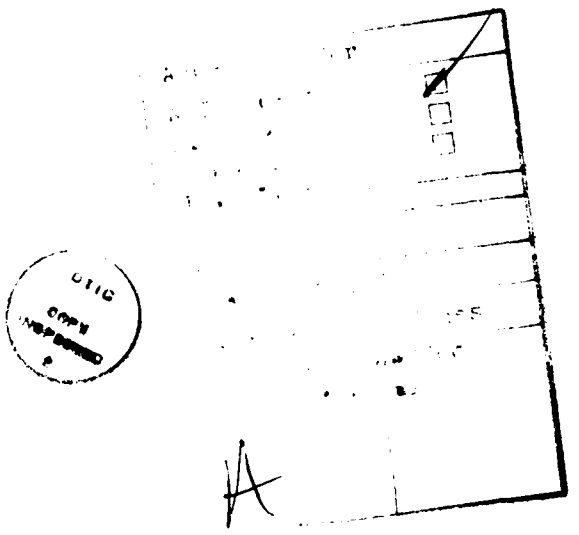

INTRODUCTION

For many years, alumina (Al_2O_3) has been recognized as a potentially promising metal matrix composite reinforcement for high-temperature and many chemically-aggressive environmental applications.[1,2] For temperatures below 900°C, it retains most of its elastic stiffness, structural strength, and abrasion resistance. It is also inert to most metals and exhibits excellent oxidation resistance.

Early attempts to utilize alumina fibers were not commercially successful due primarily to insurmountable fabrication costs and handling problems associated with the single crystal filaments and whiskers that were available at the time.[3] However, in 1975 these barriers were essentially removed by DuPont with the introduction of continuous polycrystalline alumina filaments called Fiber FP. These filaments, which are available in a multifilament yarn, can be easily fabricated into a metal matrix composite using conventional casting and liquid infiltration techniques. Because of its potential low cost,[4] the polycrystalline alumina fiber is competitive with other high performance fibers such as boron, graphite, and silicon carbide.

Aluminum[3,5] and magnesium[6] alloys have been successfully reinforced with polycrystalline alumina and are currently being evaluated for applications requiring cost-effective material property improvements. These composites have excellent compressive properties and exhibit transverse tensile strengths that are 3 to 5 times greater than similar composites reinforced with graphite.[7] However, because of high density (3.9 g/cm^3) and a moderate tensile strength (200 ksi to 270 ksi for 1-inch gage lengths) the polycrystalline alumina fiber does not compete favorably with boron or graphite for simple uniaxial-tensile applications.

All of the technically important metal matrix reinforcing fibers including alumina, boron, graphite, and silicon carbide are intrinsically brittle materials that exhibit significantly large variabilities in strength. Because of this, their failure strengths can only be statistically defined. Typically, the coefficients of variation in the mean failure strengths of these materials are 10 percent to 30 percent or higher.[8-10] In contrast, metal filaments exhibit a much lower variability in failure strength because of their ductile nature. A heavily cold-worked 304 stainless steel filament (27 μm diameter), for example, exhibits less than 5 percent coefficient of variation at a 340 [illegible] mean failure stress. This variability in strength primarily reflects the flaw sensitivity of these materials. Also, because of the probability of finding critical flaws increases as their length increases, these

1. SUTTON, W. H., and CHORNE, J. *Potential of Oxide-Fiber Reinforced Metals.* Fiber Composite Materials, Am. Soc. for Metals, Metals Park, Ohio, 1965, p. 173-222.
2. BAILEY, J. E., and BARKER, H. A. *Trial of Strength.* Chemistry in Britain, December 1974, p. 465-470.
3. PREWO, K. M. *Fabrication and Evaluation of Low Cost Alumina Fiber Reinforced Metal Matrices.* United Technologies Research Center, East Hartford, Connecticut, Contract N00014-76-C-0035, Interim Technical Report R77-912245-3, May 1977.
4. *Commercial Opportunities for Advanced Composites.* A. A. Watts, ed., ASTM STP 704, ASTM, Philadelphia, Pennsylvania, 1980.
5. CHAMPION, A. R., et al. *Fiber FP Reinforced Metal Matrix Composites.* Proceedings of the International Conference on Composite Materials, B. Norton, et al., ed., Met. Soc. of AIME, 1978, p. 883-904.
6. DHINGRA, A. K., and KRUEGER, W. H. *New Engineering Material - Magnesium Coating Reinforced with DuPont Continuous Alumina Fiber FP.* Presented at the World Conference on Magnesium, Oslo, Norway, June 1979.
7. DOW, N. F., and DERBY, F. *Survey of Metal-Matrix Technology for Fabrication of Bridging Structures.* Materials Sciences Corp., Blue Bell, Pennsylvania, Contract DAAG46-79-C-0067, Final Report, AMMRC TR 80-53, November 1980.
8. AHMAD, I., et al. *Silicon Carbide Filaments as Reinforcements for High Temperature Alloy Materials.* ICCM, Proceedings of the 1975 International Conference on Composite Materials, F. Scala, et al., ed., Met. Soc. of AIME, New York, 1976, p. 85-102.
9. STREET, K. N., and FERTE, J. P. *On the Strength-Length Dependence of Boron Fibres.* ICCM, Proceedings of the 1975 International Conference on Composite Materials, F. Scala, et al., ed., Met. Soc. of AIME, New York, 1976, p. 137-163.
10. JONES, J. B., et al. *Analysis of Flaws in High Strength Carbon Fibers from Mesophase Pitch.* J. of Materials Science, v. 15, 1980, p. 2455-2465.

filamentary materials exhibit a decrease in strength with increasing gage length. Typical examples of this strength versus gage length dependence are shown in Figures 1 and 2 for boron,[9] graphite,[10,11] silicon carbide,[8] and for comparison a heavily cold-worked 304 stainless steel. The PAN base graphite fiber (mean strengths and mean gage lengths) shown in Figure 1 were derived from individual test data reported in Reference 11.

Because of the limited amount of data available on Fiber FP (polycrystalline alumina)[3,5] an experimental study was conducted to define the gage length dependence and the statistical strength of this material. These results were then used to predict the failure strengths of uniaxially reinforced FP/aluminum and FP/magnesium composites with an analysis proposed by Zweben.[12]

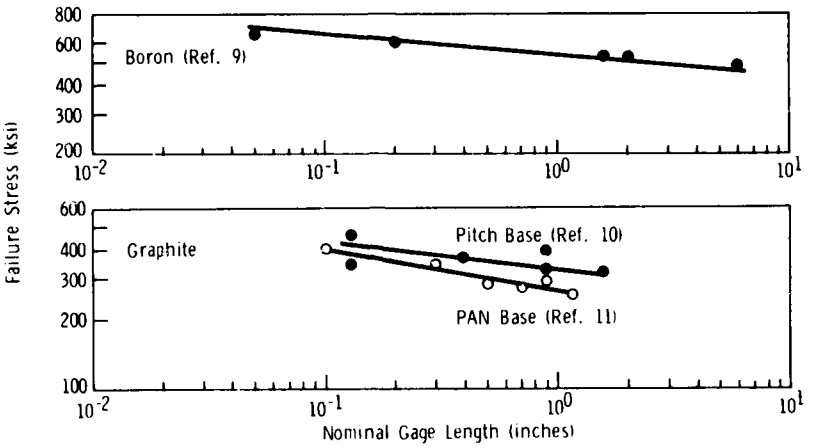

Figure 1. The effect of gage length on filament tensile failure stresses of boron and graphite.

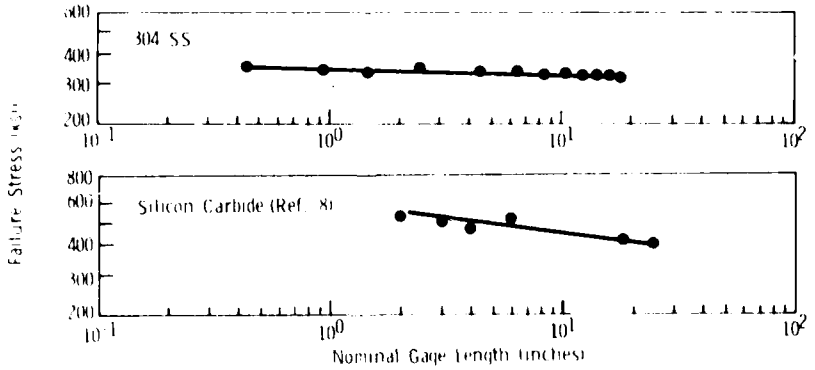

Figure 2. The effect of gage length on filament tensile failure stresses of 304 stainless steel and silicon carbide.

11. DIEFENDORF, R. J., and TAKARSKY, T. *High Performance Carbon Fibers.* Polymer Engineering and Science, v. 15, no. 3, 1975, p. 150-159.

12. ZWEBEN, C., et al. *Test Methods for Fiber Tensile Strength, Composite Flexural Modulus, and Properties of Fabric-Reinforced Laminates.* Composite Materials: Testing and Design (Fifth Conf.), ASTM STP 674, S. W. Tsai, ed., Am. Soc. for Testing Materials, 1979, p. 228-262.

EXPERIMENTAL PROCEDURE

The polycrystalline alumina used in this study was obtained from a single bobbin of Fiber FP yarn containing approximately 197 filaments purchased from DuPont. These filaments have a circular cross section and do not vary appreciably in diameter along their length. Typical SEM views of the "as-received" filaments (Figure 3) illustrate this diameter uniformity. Also shown is an organic residue that was found on most of the fiber surfaces examined. The residue is probably an acrylic that is used by DuPont in its fabrication process and can be easily burned off without damaging the filament. It was necessary to remove this residue in order to minimize filament breakage during the separation of individual filaments from the yarn.

Optical microscopic diameter measurements were obtained from metallographically mounted and polished cross sections and from longitudinal surveys of individual test specimens. The average of 54 fiber diameter measurements obtained from 1,000 magnification photomicrographs of the mounted yarn cross sections was 19.6 μm (0.772 x 10^{-3} inches) with an 8.9 percent coefficient of variation. The average of 186 diameter measurements made from longitudinal filament surveys at 660 magnification with a calibrated filar eyepiece micrometer was 20.4 μm (0.803 x 10^{-3} inches) with an 8.0 percent coefficient of variation. These results are in agreement with the 20 μm (0.787 x 10^{-3} inches) mean diameter specified by DuPont.

Filament tensile specimens were individually mounted on paper tabs to facilitate gripping and minimize grip failures. The tabs were made by cutting narrow slots equal to the fiber gage lengths in strips of paper, 1-inch wide and 1-inch longer than the slots. Each filament was placed along the center of the slot and secured at each end of the tab with adhesive tape. The specimen mounting method,

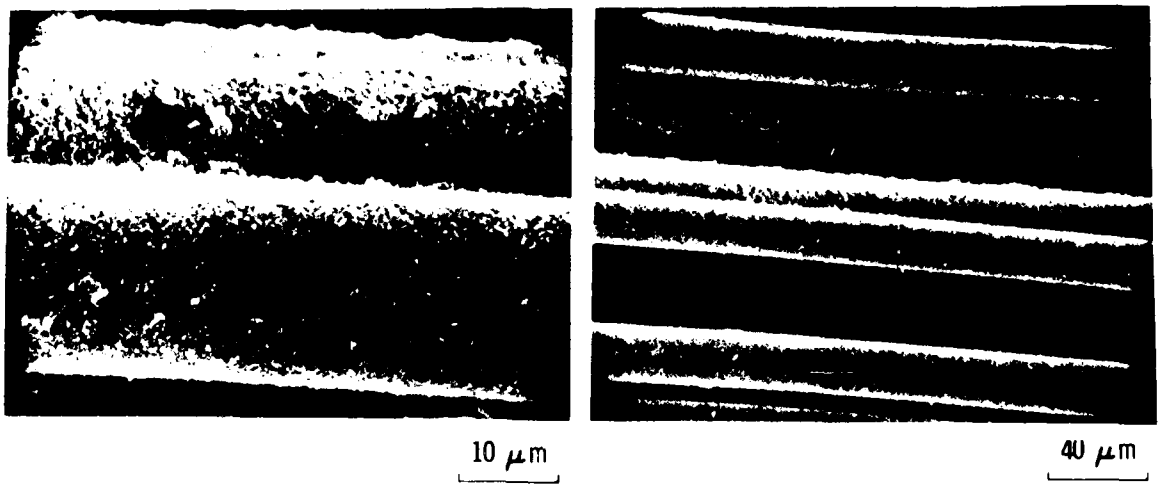

Figure 3. As-received polycrystalline alumina fibers illustrating diameter uniformity and evidence of organic residue along the surface.

as well as the testing procedure used, were similar to that specified in the ASTM standard D3379-75, "Tensile Strength and Young's Modulus for High Modulus Single Filament Materials."

After gripping both tabbed ends of the mounted specimen in the tensile machine and before applying any load, the side strips supporting the fiber were severed. The test was then performed at a constant crosshead rate of 0.2 inch per minute. During the test, tensile loads to failure were recorded using a full scale range of 100 grams (500 gram capacity load cell) at a chart speed of 10 inches per minute. A minimum of 30 filaments was tested with gage lengths of 0.5, 1, 2, 3, 5, and 10 inches.

ELASTIC MODULUS

The static elastic modulus test method[13] utilizes crosshead deflections measured for several different gage lengths at a constant stress to determine a unique tensile strain. From the constant elastic stress level chosen and the corresponding tensile strain measured, the elastic modulus can then be directly calculated.

Experimentally measured crosshead deflections, δ_t, obtained in the tensile test may be expressed as

$$\delta_t = \delta_n + \delta_c + \delta_m \qquad (1)$$

where δ_n = the deflection due to the gage length, ℓ_n; δ_c = the deflection due to the grip penetration length, ℓ_c; and δ_m = the deflection due to the load weighing system and the grips. Assuming δ_c and δ_m are constant for constant loads and are independent of gage length, the equation for δ_t may be rewritten as

$$\delta_t = \epsilon \ell_n + \delta_o \qquad (2)$$

where ϵ = the filament tensile strain. It is obvious that for constant stress, δ_t is a linear function of ℓ_n whose slope is ϵ. Summarized in Table 1 are the experimental δ_t data that were obtained at an extrapolated tensile stress of 453.2 ksi which corresponds to a 100 gram constant load. A least squares fit of these data (Figure 4) gave the following slope and intercept values:

$\epsilon = 8.07 \times 10^{-3}$ inches, and
$\delta_o = 5.24 \times 10^{-3}$ inches.

Using the above strain, a static elastic modulus of 56.2×10^6 psi was calculated which is within the range of a recently reported[14] value from DuPont of $58.2 \pm 2.6 \times 10^6$ psi.

Assuming the load cell deflection was the only factor contributing to δ_m, it was also possible to obtain the grip penetration length, ℓ_c, whose absolute value could then be used to derive a better estimate of the actual fiber gage length, ℓ_f.

13. NUNES, J., and KLEIN, W. *A Method for Determining Tensile Strains and Elastic Moduli of Metallic Filaments.* Trans. of ASM, v. 60, 1967, p. 726-727.

14. HACK, J. E., and STREMPEK, G. C. *Fabrication and Evaluation of Low Fiber Content Alumina Fiber/Aluminum Composites.* Fiber Materials Inc., Biddeford, Maine, Contract NAS3-21371, Final Report CR-159517, June 1980.

Table 1. CROSSHEAD DEFLECTIONS, δ_t, OBTAINED FOR VARIOUS POLYCRYSTALLINE ALUMINA FIBER - NOMINAL GAGE LENGTHS

Series	ℓ_n (in.)	N	δ_t* (10^{-3} in.)	Std. Dev. (10^{-3} in.)
FP-1	0.5	36	9.8	1.7
FP-7	0.5	37	9.5	1.6
FP-2	1.0	31	14.7	1.3
FP-3	2.0	33	21.3	2 5
FP-4	3.0	29	28.2	3.3
FP-5	5.0	28	45.7	5.0
FP-5A	5.0	31	43.4	6.6
FP-6	10.0	27	87.2	13.6

*δ_t was obtained by extrapolating the linear elastic load-deflection curve to 100 grams and measuring the corresponding deflection.

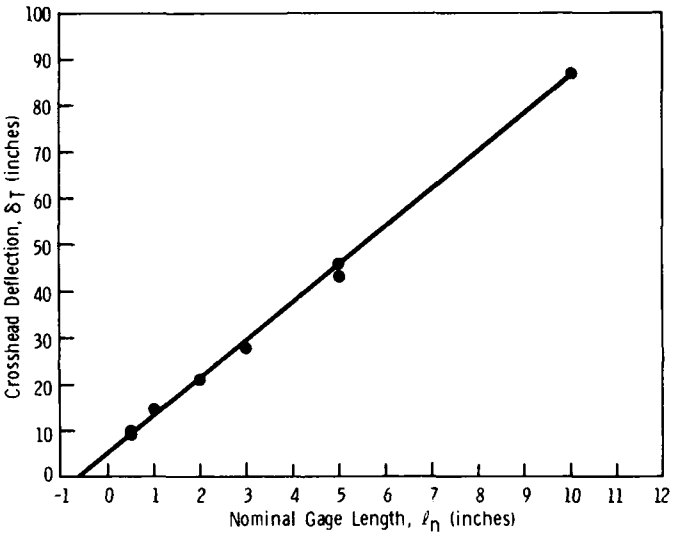

Figure 4. Crosshead deflection, δ_T, versus nominal gage length, ℓ_n, of polycrystalline alumina fibers. (Based on extrapolated elastic tensile load of 100 grams.)

$\delta_m = 3.0 \times 10^{-3}$ inches at a 100 gram load,
$\delta_c = \delta_o - \delta_m$,
$\ell_c = |0.28|$ inch
(by definition $\delta_c = \epsilon \ell_c$), and
$\ell_f = \ell_c + \ell_n$.

An accurate determination of the fiber gage length becomes critical at the shorter nominal gage lengths; e.g., the zero nominal gage length is actually a true gage length of 0.28 inch for the polycrystalline alumina filaments tested.

In order to obtain a second independent measurement, the elastic modulus was determined dynamically using a sonic pulse test method. The sonic velocity, C, was determined at an excitation frequency of 5 kHz on several individual filaments. A dynamic tensile elastic modulus, E_d, of $(57.1 \pm 3.1)10^6$ psi was calculated from the following equation using a density, ρ, of 3.90 g/cm^3:[5,6]

$$E_d = \rho c^2. \quad (3)$$

Both static and dynamic moduli agree within 2 percent of each other.

All of these moduli values, including the recently reported DuPont data, are higher than what had been published earlier[5,6] and may be indicative of further elastic property improvements.

FILAMENT TENSILE STRENGTHS

Filament tensile strengths were determined both directly and indirectly. The indirect method involved dividing the mean breaking load, $\bar{L}$, obtained for each gage length by a representative fiber area to find the mean failure stress, $\bar{\sigma}_m$. In filament testing, this is the method usually employed by investigators.

The direct method uses the individual filament area and breaking load to determine the failure stress, σ_f, and subsequently the mean failure stress, $\bar{\sigma}_f$, of all the specimens tested. For statistical failure analysis of brittle fibers, the direct method of determining failure stress is preferred, particularly when large diameter variations are present. The importance of examining each filament was further demonstrated by the discovery of "crooked" fibers in each population tested.

Typically the "crooked" filaments failed at very low loads at one of the bent sections (Figure 5) due to the superimposed bending stresses that developed in those areas. Similar observations for this type of failure with Fiber FP were made by Prewo.[3] Examination of both straight and "crooked" fiber breaks did not reveal any differences in fracture surface appearance. However, most of the fracture surfaces examined appeared to be granular (Figure 6) which would indicate a predominantly intergranular failure mode.

Listed in Table 2 are all the $\bar{\sigma}_m$ and $\bar{\sigma}_f$ filament test data obtained and the corrected gage lengths, ℓ_f, tested. Very large standard deviations (25 percent to 45 percent coefficient of variation) for both $\bar{\sigma}_m$ and $\bar{\sigma}_f$ are evident. As with other brittle filaments, the polycrystalline alumina also exhibited a strong gage length dependence with failure stress. This is shown in Figure 7 for $\bar{\sigma}_m$ versus the corrected gage length, ℓ_f.

Using Weibull statistics,[15,16] Coleman[17] proposed the following equation for describing the filament gage length mean failure stress dependence:

$$\bar{\sigma}_f = \sigma_o \ell_f^{-1/m} \Gamma [1 + 1/m] \quad (4)$$

where

$\bar{\sigma}_f$ = mean failure stress,

ℓ_f = gage length,

σ_o = normalizing constant,

m = flaw sensitivity constant, and

Γ = gama function.

15. WEIBULL, W. *A Statistical Distribution Function of Wide Applicability.* J. Appl. Mech., v. 18, 1951, p. 293-297.
16. DeSALVO, G. J. *Theory of Structural Design Application of Weibull Statistics.* Westinghouse Electric Corp., Astronuclear Lab, Pittsburgh, Pennsylvania, Report WANL-TME-2688, 1970.
17. COLEMAN, B. D. *On the Strength of Classical Fibers and Fiber Bundles.* J. Mech. and Phy. Solids, v. 7, 1958, p. 60-70.

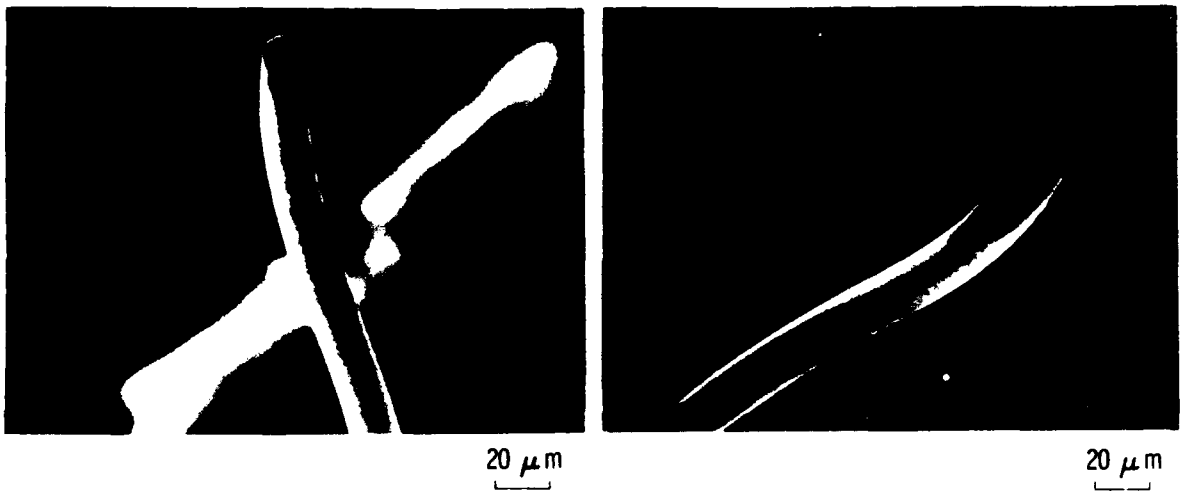

Figure 5. "Crooked" polycrystalline alumina fibers after tensile failure.

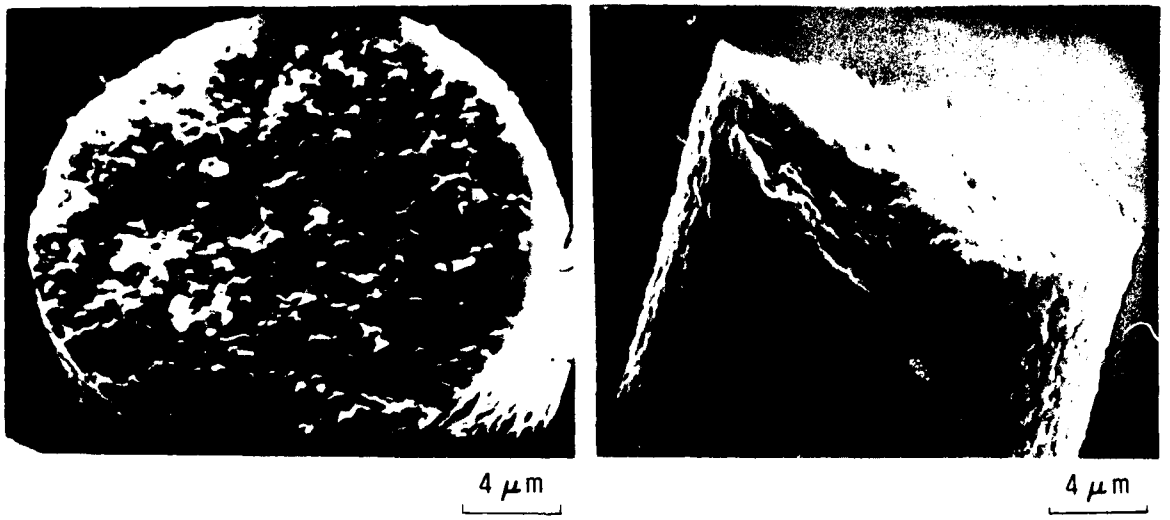

Figure 6. Typical granular fracture surface appearance for polycrystalline alumina.

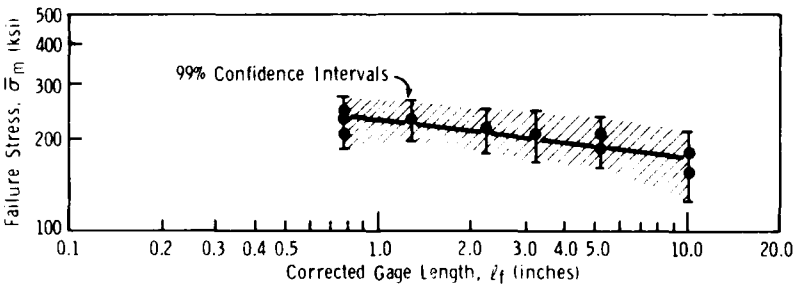

Figure 7. The effect of gage length on filament tensile failure stresses of polycrystalline alumina.

Table 2. MEAN TENSILE STRENGTH RESULTS OBTAINED ON VARIOUS POLYCRYSTALLINE ALUMINA FIBER - CORRECTED GAGE LENGTHS

Series	ℓ_f (in.)	N	$\bar{d}_f$ (10^{-3} in.)	Std. Dev. (10^{-3} in.)	$\bar{L}$ (grams)	Std. Dev. (grams)	$\bar{\sigma}_m$ (ksi)	Std. Dev. (ksi)	$\bar{\sigma}_f$ (ksi)	Std. Dev. (ksi)
FP-1	0.78	36	*	*	44.9	11.1	211.5	52.3	*	*
FP-7	0.78	44	0.797	0.058	55.2	17.8	243.9	78.6	242.2	65.4
FP-8	0.78	45	0.802	0.062	54.8	18.6	239.1	81.2	235.7	67.2
FP-2	1.28	34	*	*	49.3	16.8	232.2	79.1	*	*
FP-3	2.28	34	*	*	45.6	14.8	214.8	69.7	*	*
FP-4	3.28	33	*	*	44.2	16.5	208.2	77.7	*	*
FP-5	5.28	31	*	*	44.0	13.2	207.2	62.2	*	*
FP-9	5.28	47	0.791	0.064	42.0	14.1	188.4	63.2	187.8	59.5
FP-6	10.28	33	*	*	38.5	16.1	181.3	75.8	*	*
FP-10	10.28	40	0.824	0.074	37.7	16.9	155.8	69.9	150.6	55.4

*$\bar{d}_f = (0.772 \pm 0.069)10^{-3}$ in. Average diameter based on metallographic measurements of 54 filaments.

N = Number of filaments tested.

$\bar{d}_f$ = Average filament diameter.

$\bar{L}$ = Average filament breaking load.

$\bar{\sigma}_m$ = Average filament failure stress (indirect method).

$\bar{\sigma}_f$ = Average filament failure stress (direct method).

σ_f = Individual filament failure stress.

Many different types of fiber materials can be adequately represented by Equation 4. For comparative purposes, graphically determined values of σ_o and m are listed in Table 3 for the materials shown in Figures 1 and 2.

The flaw sensitivity constant, m, reveals the degree of flaw homogeneity or distribution which is related to the scatter exhibited in the filament test results. High m values signify a uniform distribution of very homogeneous flaws. Low m values signify a flaw severity that is highly variable or a nonuniform dispersion of flaws. Brittle materials characteristically have low m values while tougher materials, such as 304 stainless steel, exhibit much higher m values. As m approaches infinity, the scatter approaches zero and the normalizing constant, σ_o, can then be used to obtain the flaw free failure stress. This stress is not necessarily the ideal strength of the filament; rather it is the volume or surface area independent failure stress

Table 3. TYPICAL WEIBULL CONSTANTS FOR VARIOUS FILAMENTS

Material	σ_n (ksi)	σ_o (ksi-in.$^{1/m}$)	m
304 SS	345	350	40
Boron	530	556	11.4
Silicon Carbide	600	639	7.6
Graphite (Pitch Base)	325	346	7.6
Graphite (Pan Base)	260	281	5.6

σ_n = Mean failure stress at ℓ_n = 1 in.

σ_o = Normalizing constant

m = Flaw sensitivity constant

In Equation 4, it was assumed that the following two-degree-of-freedom (σ_o and m) Weibull distribution function adequately described the failure probability of most filaments.

$$P = 1-\exp\left[-\ell_f\left(\frac{\sigma_f}{\sigma_o}\right)^m\right] \tag{5}$$

For a given fracture stress, σ_f, Weibull determines the failure probability as

$$P = \frac{n}{N+1} \tag{6}$$

where n = number of filaments that fail at or below σ_f, and
N = total number of filaments tested.

A graphical solution of σ_o and m can be obtained by plotting the following linearized function of Equation 5.

$$\ell n\ \ell n\left(\frac{1}{1-P}\right) = m\ \ell n\ \sigma_f + \ell n\left(\frac{\ell_f}{\sigma_o{}^m}\right) \tag{7}$$

Using Equation 7, the failure probabilities were plotted versus σ_f for filament tensile test results obtained on 0.5-, 5.0-, and 10.0-inch nominal gage lengths (Figures 8 through 11). Weibull probability has been used to show the failure probability percentages, rather than the actual logarithmic values. The individual data points have also been tabulated in the Appendix. Two sets of data are shown in Figures 8 through 11 which represent (a) all test results including straight and "crooked" filaments, and (b) test results only for the straight filaments. As mentioned earlier, each of the gage lengths tested contained "crooked" filaments (approximately 12 percent). Because the "crooked" filaments could fail under a superimposed bending stress, they would not reflect the uniaxial tensile strength population and would not be representative of the filaments' in situ composite behavior. All of the figures show that a reasonable linear fit to the data was obtained when the suspected filaments were excluded from the distribution. Weibull parameters, σ_o and m, obtained from these linearized curves are summarized in Table 4 with the corresponding mean failure stresses. A least squares fit of $\bar{\sigma}_f$ versus ℓ_f (Figure 12) gave an m of 6.5 and σ_o of 266.9 ksi-in.$^{1/m}$ which compares favorably with the constant gage length, measurements of m and σ_o.

Table 4. WEIBULL PARAMETER AND MEAN FAILURE STRESSES FOR POLYCRYSTALLINE ALUMINA, EXCLUDING "CROOKED" FILAMENT DATA

Series	ℓ_f (in.)	N	d_f (10^{-3} in.)	L (grams)	σ_m (ksi)	Std. Dev. (ksi)	σ_f (ksi)	Std. Dev. (ksi)	σ_o (ksi-in.$^{1/m}$)	m
FP-7	0.78	39	0.804	60.2	261.4	54.3	260.2	42.9	268.0	6.8
FP-8	0.78	40	0.806	59.2	255.8	60.5	253.8	42.3	260.0	6.6
FP-9	5.28	43	0.795	44.9	199.4	48.0	200.2	45.0	298.4	5.3
FP-10	10.28	35	0.830	42.2	171.9	50.9	168.1	30.4	265.0	6.2

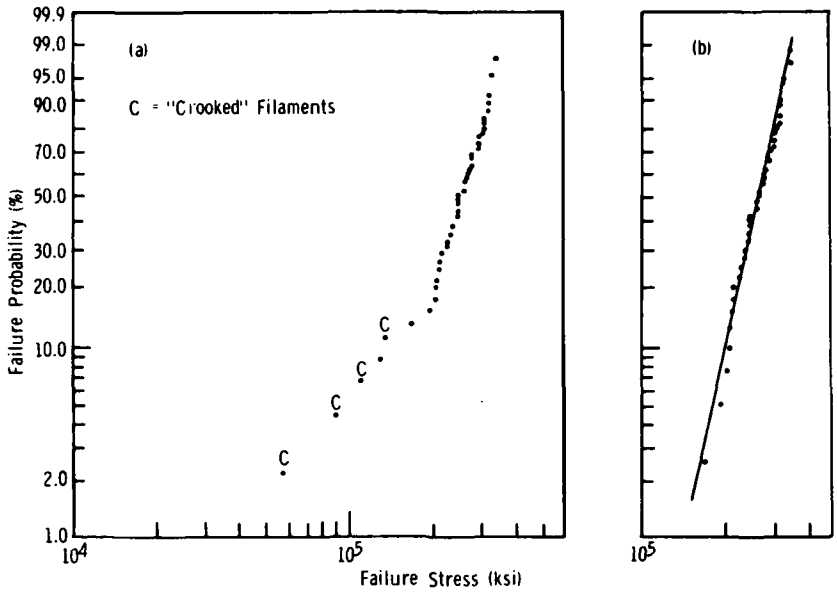

Figure 8. Weibull distribution curves for 0.5-inch nominal gage length, polycrystalline alumina filaments (FP-7 series); (a) results for all filaments tested, and (b) results with suspected filaments excluded.

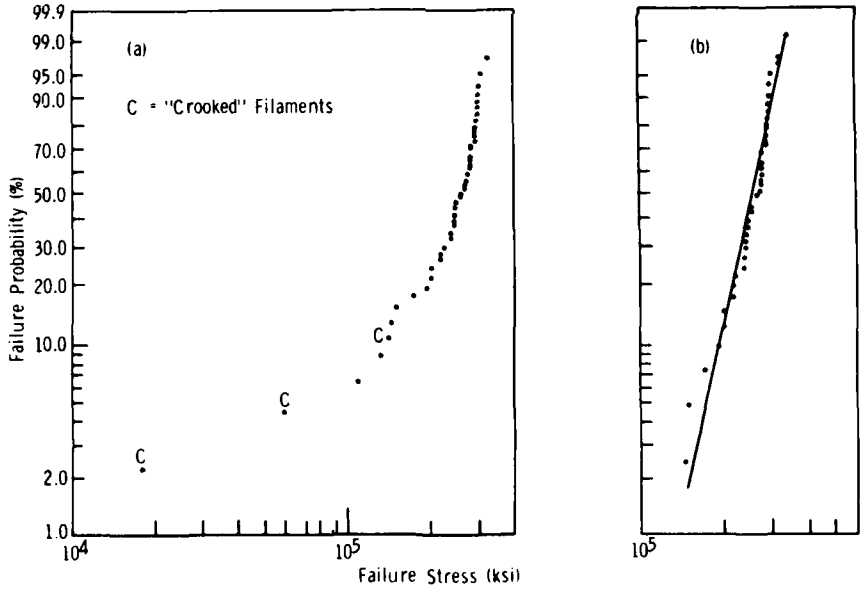

Figure 9. Weibull distribution curves for 0.5-inch nominal gage length, polycrystalline alumina filaments (FP-8 series); (a) results for all filaments tested, and (b) results with suspected filaments excluded.

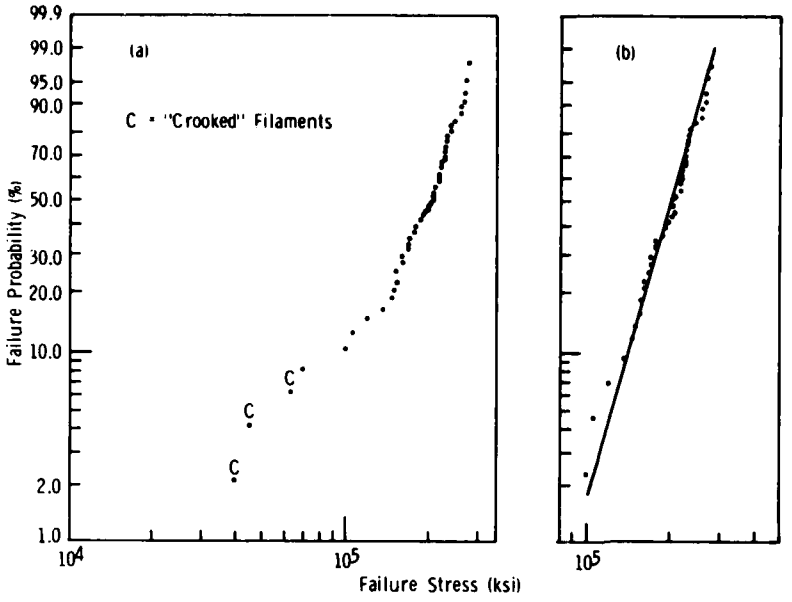

Figure 10. Weibull distribution curves for 5.0-inch nominal gage length, polycrystalline alumina filaments (FP-9 series); (a) results for all filaments tested, and (b) results with suspected filaments excluded.

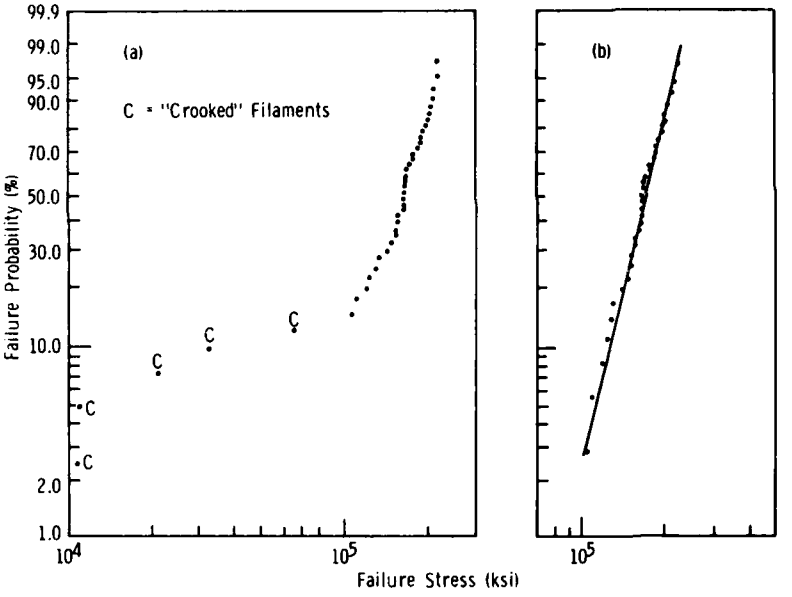

Figure 11. Weibull distribution curves for 10.0-inch nominal gage length, polycrystalline alumina filaments (FP-10 series); (a) results for all filaments tested, and (b) results with suspected filaments excluded.

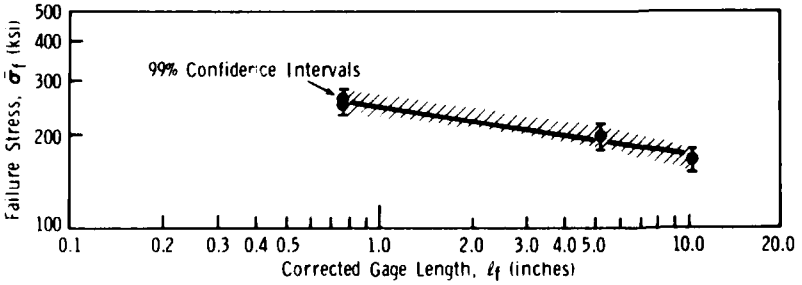

Figure 12. The effect of gage length on filament tensile failure stresses of polycrystalline alumina excluding "crooked" filaments.

COMPOSITE TENSILE STRENGTHS

A number of failure mechanisms have been proposed[12,18-20] to describe the fracture of continuous uniaxially aligned fiber-reinforced composites. At least three failure modes have been recognized for the case of tensile deformation along the fiber axis. The failure modes and several relationships that have been developed for brittle fibers using Weibull failure statistics (Equation 5) are as follows:

1. A bundle fracture mode that is characterized by very weak or no interfacial bonding between fiber and matrix. When this condition is present the composite tensile strength is controlled by the bundle strength of the fiber. The following equation by Coleman[17] describes the mean bundle strength $\bar{\sigma}_b$ for brittle filaments:

$$\bar{\sigma}_b = \sigma_o\left(\ell_f mc\right)^{-1/m} \tag{8}$$

where ℓ_f = gage length, and e = Naperian base number.

2. A transverse cracking mode that is characterized by a crack propagating from the site of the first fiber that fails. Zweben[21] has proposed a lower bound solution for determining the stress, $\bar{\sigma}_1$, required to break the first fiber as follows:

$$\bar{\sigma}_1 = \sigma_o\left(\frac{m-1}{N\ell m}\right)^{1/m} \tag{9}$$

where ℓ is the composite gage length and N is the total number of fibers. Although the transverse cracking mode may not be common to most composites, it appears to have occurred in some boron/aluminum systems[12,22] where the presence of very large diameter brittle fibers in a well-bonded matrix appears to have promoted this type of failure. A well-bonded, brittle-fiber, brittle-matrix composite would be the simplest case where Equation 9 could be expected to apply.

3. A statistical failure mode that is characterized by the accumulation of fiber breaks throughout the entire stressed composite volume. Zweben proposed[12,20] that the stress, $\bar{\sigma}_2$, required to break the first overstressed fiber leading to fiber break propagation is a lower bound for composites that exhibit the statistical failure mode. Random fiber breaks are assumed to develop localized stress perturbations. Stresses in the vicinity of the broken fibers are reduced over an ineffective gage length, δ.[23] Stress concentrations also develop in the unbroken surrounding fibers increasing their failure probability. Zweben proposed that these overstressed fibers subsequently trigger fiber break propagation when $\bar{\sigma}_2$ is reached. This lower bound stress relationship is

$$\bar{\sigma}_2 = \sigma_o\left[\tfrac{1}{4}N\ell\delta(k^m-1)\right]^{-1/2m} . \tag{10}$$

18. ROSEN, B. W. *Thermomechanical Properties of Fibrous Composites.* Proc. R. Soc. London, Ser. A 319, 1970, p. 79-94.
19. HALE, D. K., and KELLY, A. *Strength of Fibrous Composite Materials.* Annu. Rev. Materials Science, v. 2, 1972, p. 405-462.
20. ZWEBEN, C. *Tensile Strength of Hybrid Composites.* J. of Materials Science, v. 12, 1977, p. 1325-1337.
21. ZWEBEN, C. *Tensile Failure of Fiber Composites.* AIAA J., v. 6, 1968, p. 2325-2331.
22. ZWEBEN, C. *A Bounding Approach to the Strength of Composite Materials.* Eng. Fract. Mech., Great Britain, v. 4, 1972, p. 1-8.
23. ROSEN, B. W. *Mechanics of Composite Strengthening in Fiber Composite Materials.* American Soc. for Metals, Metals Park, Ohio, 1965, p. 37-75.

The stress concentration factor, k, is assumed to be 1.146 for a square array of fibers[24] and the ineffective gage length, δ, is obtained from the following equation proposed by Friedman;[25]

$$\delta = d_f\left[\frac{1}{2}\left(\frac{E_f}{G_m}\right)\left(V_f^{-1/2}-1\right)\right]^{1/2} \qquad (11)$$

where

d_f = fiber diameter,

E_f = fiber elastic tensile modulus,

G_m = matrix elastic shear modulus, and

V_f = volume fraction fibers.

Zweben also suggests that the following relation proposed by Rosen[23] predicts the upper bound stress, $\bar{\sigma}_u$, for composite failure by the statistical mode. In this case, stress concentrations are neglected, therefore

$$\bar{\sigma}_u = \sigma_o(\delta me)^{-1/m}. \qquad (12)$$

Although the physical significance of Equation 11 has been questioned,[19] it has been successfully used for evaluating both polymeric[12,22] and metal matrix[12] composite strengths.

Using the Weibull parameters (m = 6.5 and σ_o = 266.9 ksi-in.$^{1/m}$) determined in this study, a theoretical comparison was made between the various failure modes and experimental fiber failure stresses obtained from reinforced aluminum[5] and magnesium[6] composite tensile results. The statistical failure mode, lower bound stress, $\bar{\sigma}_2$, appears to give the best correlation with the experimental data as shown in Table 5. Although the bundle failure stress, $\bar{\sigma}_b$, also appears to correlate reasonably well, it cannot be considered valid because there was no evidence reported of fiber pullout or debonding for the composites evaluated. Both the lower bound stress, $\bar{\sigma}_1$, (transverse fracture mode) and the upper bound stress, $\bar{\sigma}_u$, (statistical failure mode) differed significantly from the experimental data. However, the attainment of $\bar{\sigma}_u$ is conceivable provided a well-bonded, fracture-resistant matrix is utilized. In the opposite sense, a well-bonded brittle matrix could conceivably have resulted in the attainment of $\bar{\sigma}_1$.

Referring to the $\bar{\sigma}_f$ data in Figure 12, it can be seen that at a 4-inch gage length a mean failure stress of 200 ksi is obtainable. Because the experimental composite test specimen gage lengths were 4 inches, this stress was used for a rule-of-mixtures strength prediction that assumed failure at a uniform fiber stress. Obviously, in this case, a rule-of-mixtures prediction based on $\bar{\sigma}_f$ would give unrealistically high composite tensile stresses.

24. HEDGEPETH, J. M., and VAN DYKE, P. *Local Stress Concentrations in Imperfect Filamentary Composite Materials.* J. Composite Materials, v. 1, 1967, p. 294-309.
25. FRIEDMAN, E. Proceedings of the 22nd Annual Conference of the Society of the Plastics Industry, Reinforced Plastics Division, Paper 4A, 1967.

Table 5. COMPARISON OF THEORETICAL BOUNDING STRESSES WITH EXPERIMENTAL COMPOSITE FIBER FAILURE STRESSES

Composite*	V_f (%)	$\bar{\sigma}_u$ (ksi)	$\bar{\sigma}_1$ (ksi)	$\bar{\sigma}_b$ (ksi)	$\bar{\sigma}_2$ (ksi)	Exp. Fiber Failure Stress† (ksi)
Al_2O_3/Al	60	479.9	38.7	138.6	150.6	148.9[5]
Al_2O_3/Mg	50	454.7	39.8	138.6	148.7	146.0[6]

*Where applicable: ℓ_f = 4 inches = ℓ

$N\ell = (V_f \upsilon_c / a_f)$

υ_c = Composite volume (0.2 in.^{3})

a_f = Fiber area ($d_f = 0.8 \times 10^{-3}$ in.)

$E_f = 57 \times 10^6$ psi

G_m (Al) = 3.4×10^6 psi

G_m (Mg) = 2.4×10^6 psi

†Experimental fiber failure stresses determined from composite and matrix tensile stresses in References 5 and 6 as follows:

σ_c (Al_2O_3/Al) = 95 ksi, σ_m = 14.2 ksi

σ_c (Al_2O_3/Mg) = 77 ksi, σ_m = 8 ksi

Fiber failure stress = $[\sigma_c - \sigma_m(1-V_f)]/V_f$

Figure 13 shows the experimental composite tensile strengths for the polycrystalline alumina (Fiber FP)/aluminum composites obtained from Reference 5 versus the volume fraction. The theoretical curve obtained from Equation 10 for $\bar{\sigma}_2$ gives excellent agreement with the data. Also shown is the rule-of-mixture curve that was derived from the 4-inch gage length data. A decrease in composite tensile strength with an increase in the composite volume tested can also be obtained from Equation 10. This is schematically shown in Figure 14 for the same composite system (Figure 13) at 50 percent volume fraction fiber.

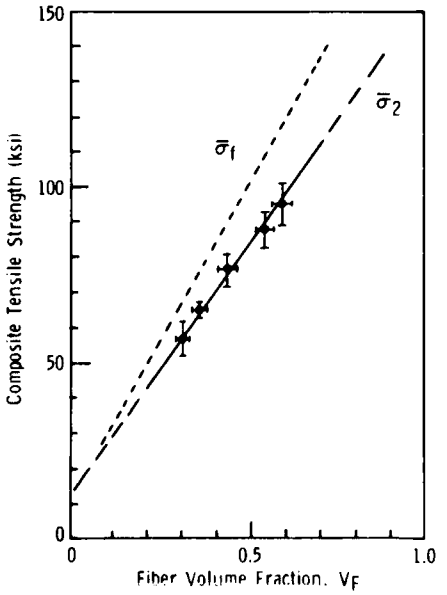

Figure 13. Experimental composite tensile strength comparisons with theoretical curves derived from the lower bound statistical failure stress, $\bar{\sigma}_2$, and the uniform failure stress, $\bar{\sigma}_f$, (4-inch gage length) for a polycrystalline alumina-reinforced aluminum alloy.

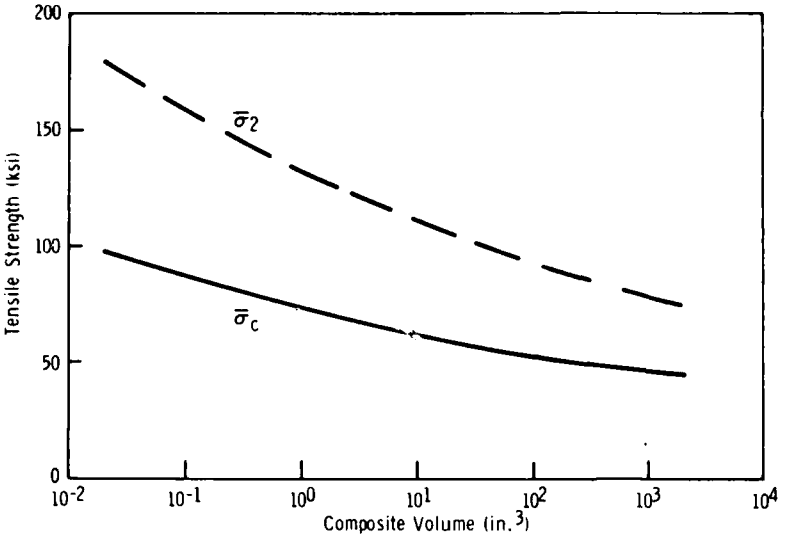

Figure 14. Schematic illustration of the theoretical effect of specimen volume on the tensile strength of a 50 percent volume fraction polycrystalline alumina-reinforced aluminum alloy. ($\bar{\sigma}_c$ is the composite strength and $\bar{\sigma}_2$ is the filament lower bound statistical failure stress.)

SUMMARY AND CONCLUSIONS

As with most brittle materials, this study has shown a significant gage length dependence and a large variability in the failure strength of polycrystalline alumina (Al_2O_3) fibers (referred to as Fiber FP by the producer, DuPont).

Some filaments in the test population contained a processing defect consisting of rigid bends along the fiber. These "crooked" filaments failed at very low loads due to the development of superimposed bending stresses at the bent sections. This change in stress state was reflected by a second linear region in the logarithmic Weibull distribution curve of failure probability versus stress.

A two-parameter Weibull distribution function was found to adequately describe the gage length dependence and failure probabilities for most of the filaments tested. (Crooked filaments were excluded from the test population as their stress state was assumed to be unrepresentative of in situ composite behavior.) The Weibull parameters that best described all the gage lengths evaluated were 6.5 for m (the flaw sensitivity constant) and 266.9 ksi-in.$^{1/m}$ for σ_o (the normalizing constant).

Exceptionally good agreement (within 2 percent) was obtained from a theoretical lower bound stress prediction based on a statistical failure mode and published tensile strength data on Fiber FP/aluminum and Fiber FP/magnesium composite castings. However, no correlation could be obtained when the same experimental data was compared to a rule-of-mixtures prediction based on the mean fiber failure stress. This further demonstrated the importance of obtaining accurate statistical strength data when dealing with brittle fiber reinforcements. Also inherent in the statistical failure mode, lower bound stress analysis, is a composite volume-failure stress dependence. Additional experimental studies are needed to confirm this analysis as well as establish the actual volume sensitivity for this type of material. Particular emphasis should be directed toward the metal matrix composite systems currently being evaluated for helicopter and bridging applications.

APPENDIX

Table A-1. FILAMENT TEST DATA FOR 0.5-INCH NOMINAL GAGE LENGTH POLYCRYSTALLINE ALUMINA (FP-7 SERIES)

Sample	d_f (10^{-3} in.)	L (grams)	σ_f (ksi)	N	P (%)
58a	0.865	90.2	338.4	39	97.5
41a	0.726	61.0	324.8	38	95.0
79a	0.855	84.6	324.8	--	--
91a	0.818	75.2	315.5	36	90.0
84a	0.717	57.6	314.5	35	87.5
42a	0.824	75.8	313.4	34	85.0
81a	0.755	62.6	308.2	33	82.5
46a	0.755	62.3	306.8	32	80.0
78a	0.824	72.8	301.0	31	77.5
77a	0.794	67.1	298.8	30	75.0
10a	0.714	52.1	292.6	29	72.5
89a	0.723	54.2	291.0	28	70.0
62a	0.816	68.8	290.0	27	67.5
65a	0.789	61.6	277.8	26	65.0
56a	0.829	67.5	275.7	25	62.5
61a	0.887	77.2	275.4	24	60.0
44a	0.776	58.0	270.4	23	57.5
49a	0.926	80.9	264.8	22	55.0
73a	0.769	55.5	263.4	21	52.5
4a	0.816	58.3	260.2	20	50.0
57a	0.717	47.5	259.4	19	47.5
51a	0.858	64.6	246.3	18	45.0
48a	0.789	54.5	245.7	17	42.5
64a	0.963	80.4	243.4	16	40.0
70a	0.782	53.0	243.3	15	37.5
37a	0.794	54.5	242.6	14	35.0
66a	0.849	62.3	242.6	--	--
59a	0.878	64.6	235.2	12	30.0
16a	0.765	47.0	230.8	11	27.5
1a	0.770	45.6	224.0	10	25.0
76a	0.801	51.0	223.1	9	22.5
3a	0.827	49.3	212.5	8	20.0
74a	0.774	45.0	210.8	7	17.5
71a	0.804	48.2	209.3	6	15.0
47a	0.823	50.0	207.2	5	12.5
11a	0.723	52.1	206.9	4	10.0
83a	0.872	54.8	202.3	3	7.5
15a	0.808	41.9	192.3	2	5.0
40a	0.794	37.5	167.3	1	2.5
17a	0.741	25.1	131.8	--	c
13a	0.751	25.2	128.5	--	c
50a	0.707	19.6	110.1	--	c
14a	0.775	17.4	87.1	--	c
18a	0.726	10.4	56.8	--	c

Table A-2. FILAMENT TEST DATA FOR 0.5-INCH NOMINAL GAGE LENGTH POLYCRYSTALLINE ALUMINA (FP-8 SERIES)

Sample	d_f (10^{-3} in.)	L (grams)	σ_f (ksi)	N	P (%)
27	0.794	71.7	319.2	40	97.6
23	0.956	97.6	299.8	39	95.1
4	0.791	66.3	297.4	38	92.7
30	0.798	67.0	295.0	37	90.2
45	0.848	75.5	294.7	36	87.8
43	0.888	82.5	293.7	35	85.4
55	0.805	67.2	291.1	34	82.9
49	0.766	60.4	289.0	33	80.5
40	0.862	76.2	287.9	32	78.0
51	0.809	67.1	287.8	31	75.6
5	0.831	70.7	287.4	30	73.2
39	0.747	57.0	286.7	29	70.7
41	0.695	48.0	278.9	28	68.3
6	0.795	62.8	278.9	--	--
44	0.875	75.8	277.9	26	63.4
24	0.842	69.9	276.8	25	61.0
15	0.874	74.8	274.9	24	58.5
37	0.737	52.6	271.8	23	56.1
38	0.768	57.0	271.3	22	53.6
3	0.795	60.8	270.0	21	51.2
19	0.788	57.9	261.7	20	48.8
25	0.835	65.0	261.7	--	--
28	0.815	60.5	255.7	18	43.9
52	0.794	57.0	253.8	17	41.5
1	0.756	49.9	245.1	16	39.0
46	0.845	62.3	244.9	15	36.5
11	0.779	52.4	242.4	14	34.1
33	0.792	54.0	241.7	13	31.7
13	0.752	48.5	240.7	12	29.3
29	0.878	65.0	236.7	11	26.8
7	0.756	48.1	236.2	10	24.4
54	0.846	56.1	220.0	9	22.0
53	0.815	50.8	214.7	8	19.5
9	0.733	41.0	214.2	7	17.1
42	0.788	44.2	199.8	6	14.6
50	0.702	35.0	199.4	5	12.2
48	0.734	36.6	190.7	4	9.8
35	1.003	61.2	170.8	3	7.3
36	0.777	32.0	148.8	2	4.9
18	0.793	31.9	142.4	1	2.4
47	0.734	26.8	139.6	--	c
12	0.724	24.4	130.7	--	c
2	0.815	25.6	108.2	--	c
16	0.826	14.0	57.6	--	c
10	0.715	3.3	18.1	--	c

Table A-3. FILAMENT TEST DATA FOR 5.0-INCH NOMINAL GAGE LENGTH POLYCRYSTALLINE ALUMINA (FP-9 SERIES)

Sample	d_f (10^{-3} in.)	L (grams)	σ_f (ksi)	N	P (%)
86	0.793	61.6	275.0	43	97.7
83	0.770	56.6	268.0	42	95.4
57	0.837	66.8	267.7	41	93.2
84	0.782	57.5	263.9	40	90.9
70	0.793	58.5	261.1	39	88.6
88	0.748	51.9	260.4	38	86.4
78	0.807	57.0	245.7	37	84.1
94	0.741	46.5	237.7	36	81.8
82	0.814	55.0	233.0	35	79.5
89	0.831	57.0	231.7	34	77.3
65	0.746	45.7	230.5	33	75.0
56	0.813	53.5	227.2	32	72.7
87	0.832	56 0	227.1	31	70.4
96	0.728	42.8	226.7	30	68.2
99	0 808	52 2	224.4	29	65.9
91	0 865	58.8	220.6	28	63.6
81	0.820	52.6	219.6	27	61.4
79	0.761	44 8	218.3	26	59.1
60	0 742	42.2	215.2	25	56.8
75	0.792	48.0	214.8	24	54.5
67	0.728	38.9	208.9	23	52.3
63	0.716	38.0	206 9	22	50.0
76	0.740	40.3	206.5	21	47.7
92	0.877	56 3	205.5	20	45.4
62	0 781	43 6	200.6	19	43.2
66	0.712	35.8	198.2	18	40.9
85	0 817	45.1	189.7	17	38.6
74	0 780	40.4	186.0	16	36.4
80	0.761	36.2	175.4	15	34.1
97	0 715	31.8	174.6	14	31.8
95	0 731	32.2	169.2	13	29.5
69	0.793	37.8	168.7	12	27.3
93	0.817	40.0	168.2	11	25.0
102	0.879	44.3	160.9	10	22.7
68	0.807	37.3	160.8	9	20.4
55	0.835	38.1	153.4	8	18.2
61	0.623	36.9	152.9	7	15.9
64	0.946	47 7	149.6	6	13.6
100	0 760	29.8	144.8	5	11.4
71	0 757	27.5	134.7	4	9.1
72	1.062	47.6	118.2	3	6.8
77	0.728	19.8	104.9	2	4.5
59	0.788	22.0	99.5	1	2.3
98	0.737	13.4	69.3	--	c
90	0.233	12.2	63.7	--	c
73	0.761	9.4	45.6	--	c
101	0.749	8.0	40.0	--	c

Table A-4. FILAMENT TEST DATA FOR 10.0-INCH NOMINAL GAGE LENGTH POLYCRYSTALLINE ALUMINA (FP-10 SERIES)

Sample	d_f (10^{-3} in.)	L (grams)	σ_f (ksi)	N	P (%)
5	0.829	54.2	221.4	35	97.2
35	0.803	50.1	218.1	34	94.4
19	0.963	70.0	211.9	33	91.7
31	0.866	55.5	207.7	32	88.9
32	0.844	51.6	203.3	31	86.1
18	0.768	42.3	201.3	30	83.3
40	0.787	44.1	199.9	29	80.6
8	0.758	40.4	197.4	28	77.8
11	0.839	47.8	190.6	27	75.0
41	0.954	61.1	188.5	26	72.2
14	1.011	68.0	186.8	25	69.5
25	0.908	53.9	183.5	24	66.7
27	0.924	54.2	178.2	23	63.9
42	0.788	39.4	178.1	22	61.1
33	0.796	38.6	171.0	21	58.3
26	0.805	39.1	169.4	20	55.6
15	0 905	49.0	167.9	19	52.8
3	0.754	33.7	166.4	18	50.0
38	0.771	35.2	166.2	17	47.2
34	0.885	46.3	165.9	16	49.4
20	0.818	39.5	165.7	15	41.7
4	0.813	39.0	165.6	14	38.9
29	0.944	51.5	162.2	13	36.1
12	0.827	37.9	155.6	12	33.3
9	0.985	53.6	155.1	11	30.6
37	0.815	35.9	151.7	10	27.8
36	0.780	32.7	150.0	9	25.0
10	0.803	33.6	146.3	8	22.2
21	0.722	26.2	141.1	7	19.4
2	0 806	29.9	131.1	6	16.7
24	0.769	27.1	128.6	5	13.9
13	0.729	23.2	122.5	4	11.1
16	0.828	29.0	118.7	3	8.3
39	0.718	20.2	110.0	2	5.5
7	0.756	21.7	106.6	1	2.8
17	0.804	15.0	65.1	--	c
22	0 778	7.0	32.5	--	c
6	0.800	4.7	20.6	--	c
23	0.774	2.3	10.8	--	c
30	0.729	2.0	10.6	--	c

DISTRIBUTION LIST

No. of Copies	To
1	Office of the Under Secretary of Defense for Research and Engineering, The Pentagon, Washington, DC 20301
12	Commander, Defense Technical Information Center, Cameron Station, Building 5, 5010 Duke Street, Alexandria, VA 22314
1	Metals and Ceramics Information Center, Battelle Columbus Laboratories, 505 Avenue, Columbus, OH 43201
	Defense Advanced Research Projects Agency, Defense Sciences Office/MSD, 1400 Boulevard, Arlington, VA 22209
1	ATTN: LTC Loren A. Jacobson
	Deputy Chief of Staff for Research, Development, and Acquisition, Headquarters, Department of the Army, Washington, DC 20310
1	ATTN: DAMA-ARZ
	Commander, Army Research Office, P.O. Box 12211, Research Triangle Park, NC 27709
1	ATTN: Information Processing Office
	Commander, U.S. Army Materiel Development and Readiness Command, 5001 Eisenhower Avenue, Alexandria, VA 22333
1	ATTN: DRCLDC
	Commander, U.S. Army Armament Research and Development Command, Dover, NJ 07801
1	ATTN: DRDAR-SCM, J. D. Corrie
1	Mr. Harry E. Pebly, Jr., PLASTEC, Director
	Director, U.S. Army Ballistic Research Laboratory, Aberdeen Proving Ground, MD 21005
1	ATTN: DRDAR-TSB-S (STINFO)
	Commander, U.S. Army Electronics Research and Development Command, Fort Monmouth, NJ 07703
1	ATTN: DELSD-L
1	DELSD-E
	Commander, U.S. Army Foreign Science and Technology Center, 220 7th Street, N.E., Charlottesville, VA 22901
1	ATTN: Military Tech, Mr. Marley
	Commander, U.S. Army Materiel Systems Analysis Activity, Aberdeen Proving Ground, MD 21005
1	ATTN: DRXSY-MP, H. Cohen
	Commander, U.S. Army Missile Command, Redstone Arsenal, AL 35809
1	ATTN: Technical Library
1	DRSMI-RLM

No. of Copies	To
	Commander, U.S. Army Research and Technology Labs, Applied Technology Laboratory (AVRADCOM), Fort Eustis, VA 23604
1	ATTN: DRDAR-ATL-ATP, Mr. James Gomez, Aerospace Engineer
	Naval Research Laboratory, Washington, DC 20375
1	ATTN: Dr. J. M. Krafft - Code 5830
1	Dr. G. R. Yoder - Code 6384
	Chief of Naval Research, Arlington, VA 22217
1	ATTN: Code 471
	Naval Sea Systems Command, Washington, DC 20362
1	ATTN: Mr. Marlin Kinna - 62R4
	Naval Surface Weapons Center, White Oak, Silver Spring, MD 20910
1	ATTN: Steven G. Fishman - Code R32
1	John V. Foltz - Code R32
	Commander, U.S. Air Force Wright Aeronautical Laboratories, Wright-Patterson Air Force Base, OH 45433
1	ATTN: AFWAL/MLSE, E. Morrissey
1	AFWAL/MLC
1	AFWAL/MLLP/D. M. Forney, Jr.
1	AFWAL/MLBC/Mr. Stanley Schulman
1	AFWAL/MLLS/Dr. Terence M. F. Ronald
	National Aeronautics and Space Administration, Washington, DC 20546
1	ATTN: Mr. B. G. Achhammer
1	Mr. G. C. Deutsch - Code RW
1	Mr. Michael A. Greenfield, Program Manager for Materials, Code RTM-6
	National Aeronautics and Space Administration, Marshall Space Flight Center, Huntsville, AL 35812
1	ATTN: R. J. Schwinghammer, EH01, Dir, M&P Lab
1	Mr. W. A. Wilson, EH41, Bldg. 4612
	The Boeing Vertol Company, P.O. Box 16858, Philadelphia, PA 19142
1	ATTN: Mr. Robert L. Pinckney, Mail Stop P62-06
1	Mr. Joseph W. Lenski, Jr., Mail Stop P32-09
	E. I. DuPont De Nemours and Company, Inc., Textile Fibers Department, Pioneering Research Laboratory, Experimental Station, Wilmington, DE 19898
1	ATTN: Dr. Blake R. Bichlmeir
1	Dr. H. J. Nusbaum
1	Mr. Jack L. Cook, Exxon Enterprises, P.O. Drawer H, Old Buncombe at Poplar, Greer, SC 29651
	Manager, Metal Matrix, AVCO Specialty Materials Division, 2 Industrial Avenue, Lowell, MA 01851
1	ATTN: Dr. James Cornie
1	Dr. Y. Murty

No. of Copies	To
1	Dr. Bhagwam K. Das, Engineering Technology Supervisor, The Boeing Company, P.O. Box 3999, Seattle, WA 98124
1	Leroy Davis, NETCO, 2225 East 28th Street, Building 5, Long Beach, CA 90806
1	Mr. Joseph F. Dolowy, Jr., President, DWA Composite Specialties, Inc., 21133 Superior Street, Chatsworth, CA 91311
1	Mr. Robert E. Fisher, President, AMERCOM, Inc., 8948 Fullbright Avenue, Chatsworth, CA 91311
1	Louis A. Gonzalez, Kaman Tempo, 816 State Street, Santa Barbara, CA 93101
1	Dr. Ernest G. Kendall, The Aerospace Corporation, P.O. Box 92957, Los Angeles, CA 90009
1	Mr. Patrick J. Moore, Staff Engineer, Lockheed Missiles and Space Company, Organization 62-60, Building 104, P.O. Box 504, Sunnyvale, CA 94086
1	Mr. Stan J. Paprocki, Material Concepts, Inc., 2747 Harrison Road, Columbus, OH 43204
1	R. Byron Pipes, Professor & Director, Center for Composite Materials, University of Delaware, Newark, DE 19711
1	Dr. Karl M. Prewo, Principal Scientist, United Technologies Research Center Mail Stop 24, East Hartford, CT 06108
1	Professor Marc H. Richman, Division of Engineering, Brown University, Providence, RI 02912
1	Mr. Robert C. Van Siclen, Vought Corporation, Advanced Technology Center, P.O. Box 226144, Dallas, TX 75266
1	Dr. Carl Zweben, General Electric Company, Valley Forge Space Center/M4018, P.O.Box 8555, Philadelphia, PA 19101
	Director, Army Materials and Mechanics Research Center, Watertown, MA 02172
2	ATTN: DRXMR-PL
1	Author


FILM